AIAA JOURNAL
Vol. 36, No. 6, June 1998

Measurement of Continuous Pressure and Shear Distributions Using Coating and Imaging Techniques

Daniel C. Reda,* Michael C. Wilder,† Rabindra D. Mehta,‡ and Gregory Zilliac§
NASA Ames Research Center, Moffett Field, California 94035-1000

The pressure-sensitive paint (PSP) method and the shear-sensitive liquid crystal coating (SSLCC) method were sequentially applied to measure the areal pressure and shear stress vector distributions on a planar test surface beneath an inclined, axisymmetric, turbulent impinging jet. The combined results provide the first-ever consolidated measurements of the continuous normal and tangential force distributions beneath a fundamental flowfield. Results indicate that the PSP method can be extended to the measurement of small pressure differences ($< \sim 0.1$ psig) encountered in low-speed atmospheric flows. Further, these results provide the first demonstration of the capability of the SSLCC method to measure continuous shear stress vector distributions on planar surfaces beneath flowfields where shear vectors of all possible orientations are present.

Nomenclature

A, B = constants in pressure-sensitive paint (PSP) calibration curve
D = jet-exit diameter
H = hue
I = intensity
I_0 = intensity, no-flow condition
L = jet pipe length
M = Mach number at jet-exit centerline
P = pressure
P_0 = stagnation pressure at jet-exit centerline; for PSP calibration, the no-flow reference pressure
P_∞ = ambient pressure
Re = Reynolds number at jet-exit centerline, based on D
X = axial coordinate on test surface
Y = transverse coordinate on test surface
α = above-plane angle, measured positive upward from zero in plane of test surface
τ = magnitude of surface shear stress vector
ϕ = circumferential angle in plane of test surface, measured positive counterclockwise from origin on negative X axis
ϕ_τ = orientation of surface shear stress vector directed away from observer with an in-plane line of sight at $\phi = \phi_\tau$

Subscripts

C = camera
J = jet

I. Introduction

In experimental fluid mechanics and aerodynamics research, one major challenge has always been to accurately measure the two surface force distributions, pressure and shear stress, acting on a given solid boundary and to accomplish such measurements with sufficient spatial detail so as to define the governing phenomenology and fundamental flow physics. Prior to the present decade, scientists and engineers had at their disposal only point-measurement methods to accomplish this goal. Recent discoveries of pressure-sensitive and shear-sensitive coatings, combined with the availability of high-resolution, light-sensing, charge-coupled device (CCD) arrays, have led to the development of full-surface pressure and full-surface shear stress vector measurement methodologies. The objective of the present research was to apply both methodologies to a common experiment, providing combined measurements of the continuous normal and tangential force distributions beneath a fundamental flowfield.

II. Experimental Arrangement

An inclined, axisymmetric, turbulent impinging jet was chosen to generate the surface pressure and shear stress vector fields. A schematic of the jet and test surface is shown in Fig. 1. The overall experimental apparatus was described previously.[1]

The jet diameter was 0.33 in., and the jet initial velocity profile corresponded to a fully developed turbulent pipe flow velocity profile with a centerline exit Mach number of 0.66. The Reynolds number, based on exit centerline conditions and exit diameter, was 1.36×10^5. The jet exhausted into atmospheric pressure, and the jet total temperature matched the ambient level.

The jet-exit plane was 13 jet-exit diameters from the geometric stagnation point (GSP), the center of the 6-in.-diam test surface. The jet-impingement angle was 57 deg relative to the plane of the disk.

Jet-impingement flows of this type are relevant to a variety of practical engineering problems and have been investigated previously using conventional point-measurement techniques[2–5] and temperature-sensitive liquid crystal coatings.[5]

The mean, time-averaged, surface streakline pattern observed beneath this flowfield is shown in Fig. 2. A very-low-viscosity liquid crystal mixture was used to generate this oil-flow pattern; the method is described in Ref. 1. The higher-viscosity liquid crystal coating used to measure the surface shear stress vector field did not flow in this manner. Such oil-flow streaklines generally are assumed to be tangential to the time-averaged local shear stress vector at every point along a given streak trajectory. As can be seen, a small, elliptically shaped stagnation zone formed at the GSP. Streaklines progressed outward from this stagnation zone in an azimuthally asymmetric pattern while maintaining a mirror-image symmetry about the X axis (the vertical centerline of this image) as dictated by the geometric arrangement.

A microtuft array was applied temporarily to the uncoated test surface in an attempt to visualize any unsteadiness in the shear vector directions. Within a circular zone of radius $\sim 3D$ centered on the GSP, tufts were seen to undergo oscillations in direction about their mean, time-averaged orientations. Tufts located outside of this jet-impingement zone were steady in orientation. The impact of such unsteadiness on both the liquid crystal coating method and the fringe-imaging skin friction technique employed to measure

Presented as Paper 97-2489 at the AIAA 32nd Thermophysics Conference, Atlanta, GA, June 23–25, 1997; received July 16, 1997; revision received Feb. 3, 1998; accepted for publication Feb. 3, 1998.

*Senior Research Scientist, Fluid Mechanics Laboratory. Associate Fellow AIAA.
†Senior Research Scientist, MCAT, Inc. Member AIAA.
‡Senior Research Scientist, Fluid Mechanics Laboratory. Member AIAA.
§Research Scientist, Fluid Mechanics Laboratory.

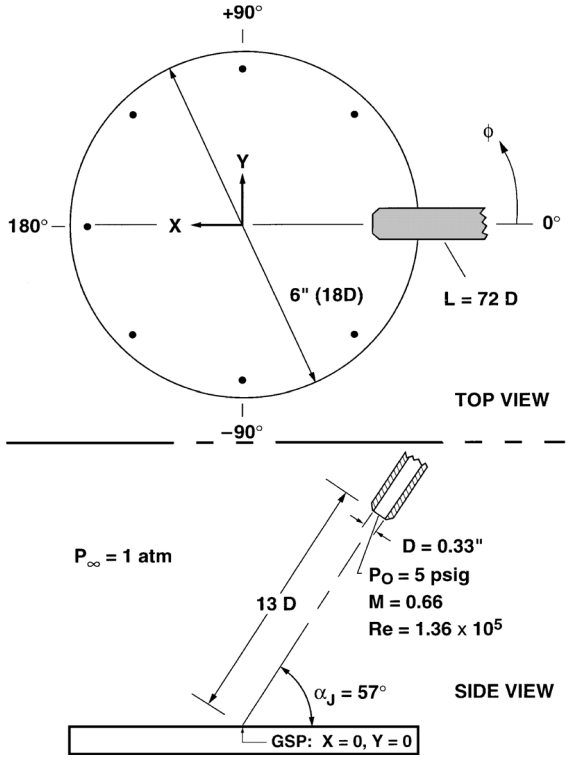

Fig. 1 Schematic of experimental arrangement.

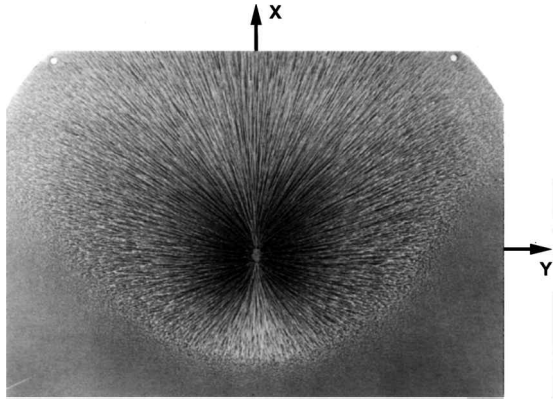

Fig. 2 Oil-flow visualization.

mean, time-averaged shear stress vector magnitudes and directions is unquantified at present.

III. Normal Force Distribution

A. Pressure-Sensitive Paint (PSP) Method

Surface pressure measurements form an integral part of all aerodynamic testing. Surface pressures are used for evaluating loads on the model; in addition, they often can reveal important details of the flowfield, such as boundary-layer separation. The conventional pressure measurement method is based on pressure taps and transducers, and although this method still is used routinely, it has several deficiencies. First, it provides measurements only at discrete points. Second, pressure-tap installation on typical models accounts for a large portion of the overall cost. Third, and most important, the overall design-cycle time is increased significantly because pressure-tap installation is both tedious and time-consuming.

A relatively new approach to the measurement of surface pressures is through the use of PSPs.[6] The model surface is coated with an oxygen-sensitive luminescent molecule dispersed in an oxygen-permeable binder and illuminated with a light of appropriate wavelength to excite the paint molecules. The excited molecules return to the ground state either by emitting light (luminescence) or through a radiationless deactivation process whereby the paint molecules lose their energy to oxygen molecules (oxygen quenching). Therefore, the intensity of the resulting luminescence is inversely proportional to the partial pressure of oxygen. Because the mole fraction of oxygen in air is a known constant, the air pressure can be determined easily once the luminescence distribution has been measured. The luminescence distribution can be measured conveniently using an imaging camera or a scanning photodiode. Thus, a complete field measurement of the pressure distribution over the whole model can be obtained readily by use of this technique.

The first application of PSPs to aerodynamic measurements was in the former Soviet Union in the mid-1980s.[7] In the Western world, the first demonstration of this method to measure continuous surface pressure distributions took place at NASA Ames Research Center in 1989 using a coating developed at the University of Washington.[8] The PSP technique now is used widely for measuring surface pressure distributions on wind-tunnel models at transonic and supersonic Mach numbers.[6]

In the present experiment, the 6-in.-diam test plate was instrumented with a single row of 15 ($\frac{1}{32}$-in.-diam) pressure taps, located along the major diameter and distributed symmetrically about the center of the disk. The tap spacing was smallest in the stagnation region of the impinging jet. This row of taps could be aligned at any angle relative to the jet axis by simply rotating the test plate.

The plate was painted with a white undercoat and a PSP (FIB 7) supplied by the University of Washington. A small amount of blowing was supplied through the pressure taps during the painting process to ensure that the taps were not blocked by the paint. A uv lamp with a wavelength centered at 365 nm was used to excite the paint. The reference (flow-off) and flow images were captured using a 14-bit Photometrics digital camera equipped with an 80-mm Nikon lens and operated through a Pentium-133 personal computer. The image data were reduced on the personal computer using MATLAB software.

The full-surface PSP data were averaged over five separate images obtained at the same time as the pressure-tap data acquisition. The pressure taps were connected to a 5-psid Setra differential pressure transducer via a manual-step scanivalve. The pressure data were acquired at a rate of 200 samples/s and averaged over 5 s.

The oxygen quenching of luminescence can be described using the Stern–Volmer[6] relation

$$I_0/I = A + B(P/P_0)$$

Here the subscript 0 denotes the value for no-flow conditions. The in situ calibration based on this equation for the present experiment is shown in Fig. 3a. It is clear that a single linear relationship did not fit the data very well. However, two linear curves with an intercept at about 0.1 psig did fit the data satisfactorily. The same trend, where two linear relationships or a single nonlinear relationship were preferable, also was observed in earlier work using a different PSP (PtOEP/GP197) (Ref. 9). In both cases, the measured pressure range was relatively small and included near-atmospheric pressures.

One potential reason for this observed dual-slope (nonlinear) behavior is the temperature sensitivity of the PSP formulation. In the present case, the recovery temperature at the GSP was estimated to be ~1°F lower than the ambient level. Recent low-speed PSP measurements[10] have shown that such very small surface temperature variations can affect PSP calibrations for cases wherein the full-scale range of pressure differences to be measured is small. However, because the temperature distribution on the test plate was not measured, temperature corrections were not attempted, and the data were reduced using the two linear relationships shown in Fig. 3a. Only 6 of the 15 pressure-tap data points were used in the calibration, together with the reference point at the origin (0,1). The two linear fits then were applied to the intensity ratio data to produce the full-surface pressure contours shown in Fig. 4a. The pressure-tap locations were filled in using an average from the surrounding pixels, and the intensity data were low-pass filtered (spatially) before applying the calibration.

B. Results

The surface-pressure contour plot of Fig. 4a shows a pressure maximum in the stagnation region followed by a rapid, azimuthally

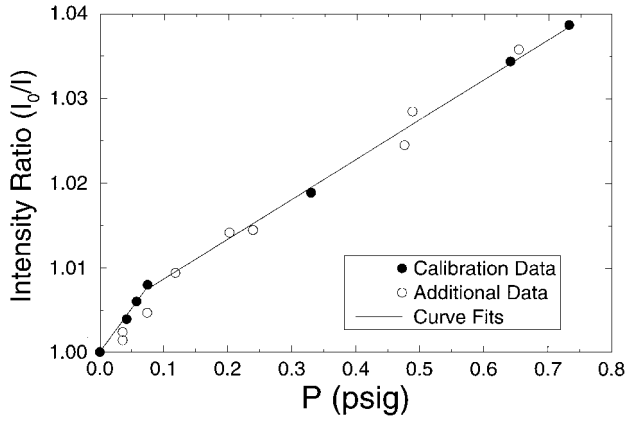

a) PSP method

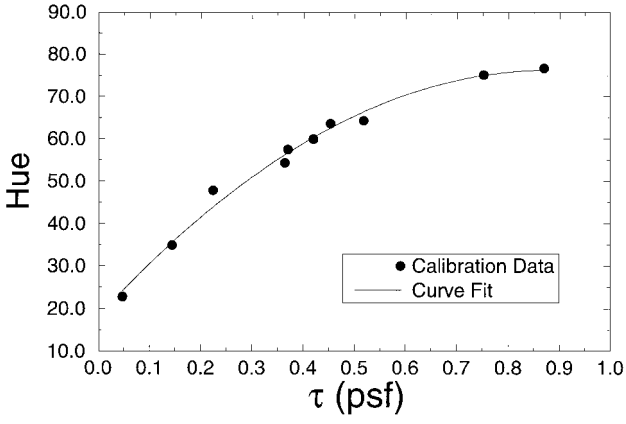

b) SSLCC method

Fig. 3 Calibration curves.

asymmetric dropoff in the radial direction. This asymmetry obviously was expected because the jet was inclined along the X axis. The pointwise and continuous pressure distributions measured along the X axis are shown in Fig. 5a. Of particular note are the tap data that were not used in the calibration. The overall agreement between the two methods was seen to be quite good, even in regions of relatively low pressure. A similar cut along the Y axis, shown in Fig. 6a, demonstrates the symmetry of the pressure distribution about the geometric plane of symmetry (the X axis). Here again, the continuous PSP pressure distribution was seen to agree quite well with the discrete pressure-tap data. Note that none of these tap data (along the Y axis) were used in the in situ PSP calibration. On average, pressures given by the PSP technique agreed with the tap data to within 2% of the maximum pressure of 0.73 psig, i.e., to within 0.015 psig.

IV. Tangential Force Distribution

A. Shear-Sensitive Liquid Crystal Coating (SSLCC) Method

The liquid crystal phase of matter is a weakly ordered, viscous, fluid-like state that exists between the nonuniform liquid phase and the ordered solid phase of certain organic compounds.[11] Liquid crystals can exhibit optical properties that are characteristic of solid, crystalline materials. If a thin film of liquid crystals is applied to a solid surface and the molecules within the coating are aligned by frictional forces into the required planar state, then this molecular arrangement selectively scatters incident white light as a three-dimensional spectrum or color space.

When the SSLCC is illuminated from the normal direction by white light and observed from an oblique above-plane view angle, its color-change response to shear depends on both shear stress vector magnitude and the direction of the applied shear vector relative to the observer's in-plane line of sight. At any point, the maximum

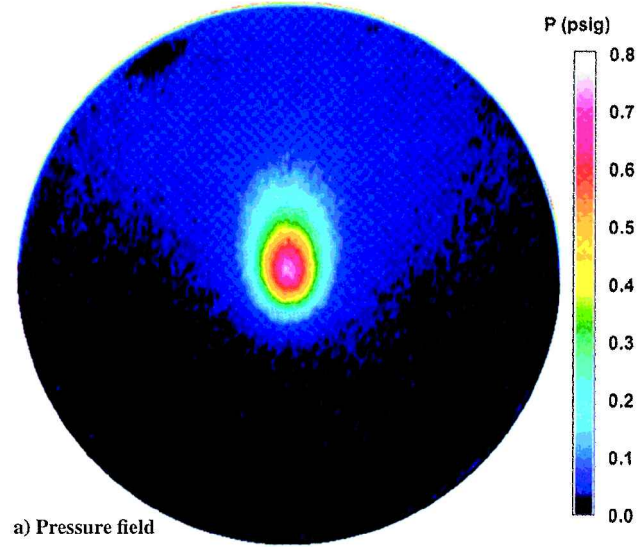

a) Pressure field

a) Pressure field

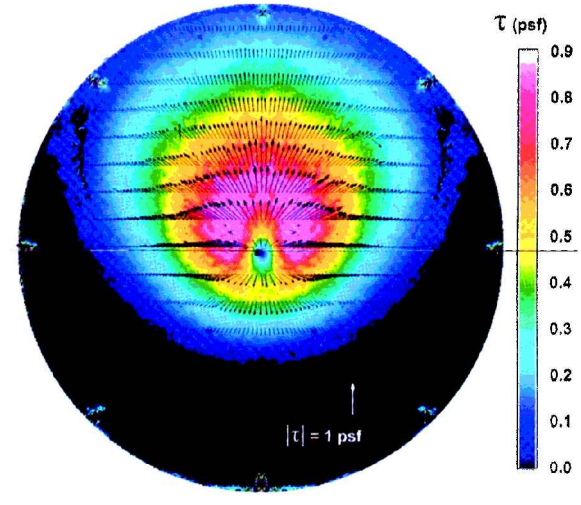

b) Shear stress vector field

b) Shear stress vector field

Fig. 4 Measured full-surface force distributions.

color change always is measured when the local shear vector is aligned with, and directed away from, the observer; the magnitude of the color change at this vector/observer-aligned orientation scales directly with shear stress magnitude.[12] Based on this knowledge, a full-surface shear stress vector measurement methodology was formulated, successfully demonstrated, and validated.[1] Reference 13 provides a demonstration of the newly discovered flow visualization capabilities of the SSLCC technique for simultaneous, full-surface observations of both transition and separation.

For full-surface shear vector measurements, a three-CCD red-green-blue (RGB) video camera, a frame grabber, and a supporting computer are utilized. The coated surface is illuminated from the normal direction, and the camera is positioned at a constant above-plane view angle, $\alpha_c \sim 30$ deg. Full-surface images of the SSLCC color-change response to an unknown shear field are recorded from multiple in-plane view angles encompassing the shear vector directions to be measured. For each physical point on the test surface, a Gaussian curve is fitted to the hue vs in-plane view angle data. The in-plane view angle corresponding to the maximum of the curve fit determines the vector orientation ϕ_τ. The vector-aligned hue value then is converted to a shear magnitude τ via a calibration curve acquired using conventional point-measurement techniques.[14,15]

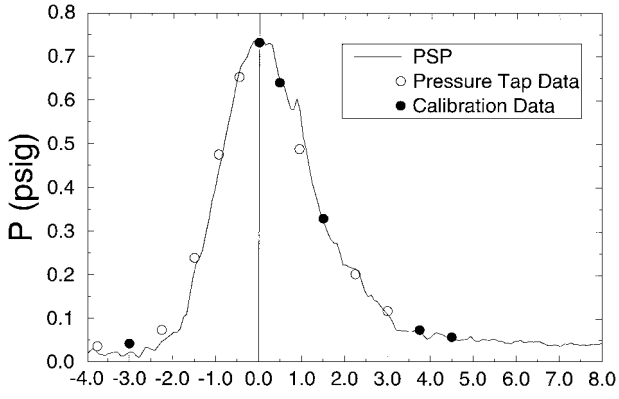

a) Pressure

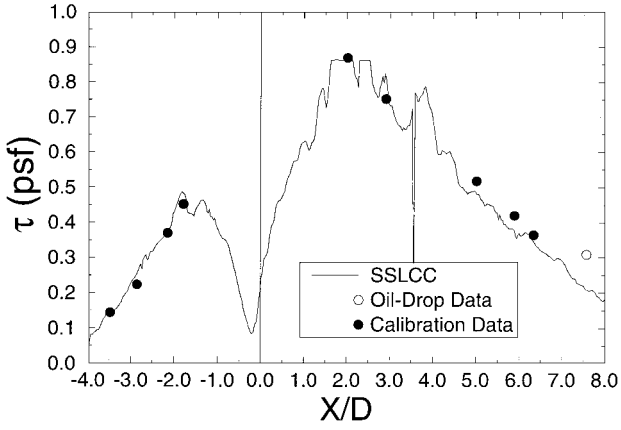

b) Shear stress magnitude

Fig. 5 Force distributions along *X* axis.

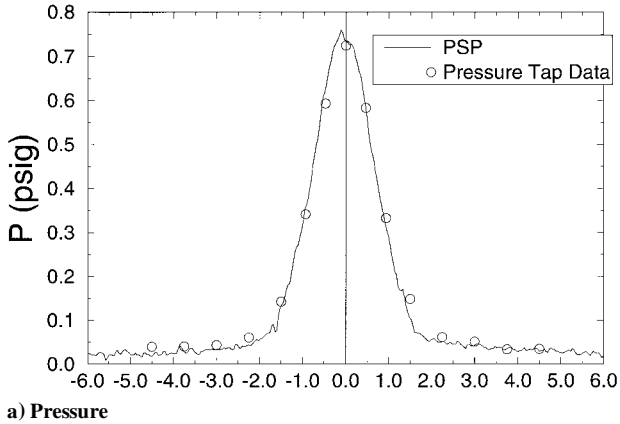

a) Pressure

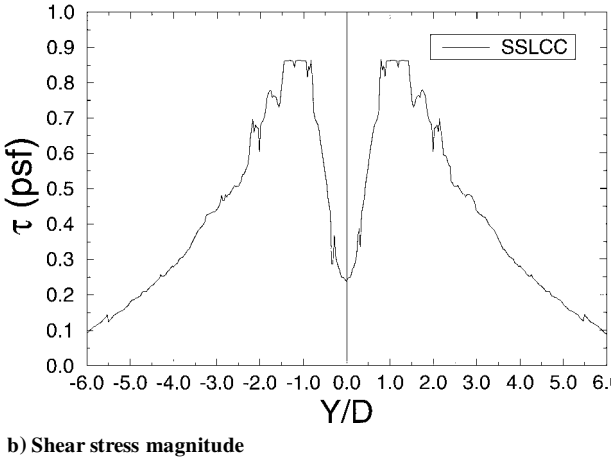

b) Shear stress magnitude

Fig. 6 Force distributions along *Y* axis.

SSLCC vector measurement resolution and accuracy issues are discussed in detail in Ref. 1. Uncertainties of 2–4% in shear vector magnitude and less than 1 deg in shear vector orientation were observed.

Hallcrest shear-sensitive liquid crystal compound BCN/192 was used for the shear vector measurements. A new coating was applied for each ϕ_c image. The camera above-plane view angle α_c was held constant at 30 deg. A 20-frame-average RGB image of the complete test surface was recorded from each of 15 ϕ_c orientations over the arc $0 \leq \phi_c \leq 180$ deg. Because of the widely varying RGB intensities experienced within each such color image, all ϕ_c images were recorded at two or more exposure settings and then mathematically combined to form a single, composite image wherein each pixel was correctly exposed. All such composite images were low-pass filtered using a 5×5 pixel mask and converted from RGB to hue-saturation-intensity (HSI) color space using the second of three hue-based trichromic systems outlined in detail by Hay and Hollingsworth.[16]

In Ref. 1, a different HSI color space was utilized, one preprogrammed by the manufacturer (Matrox) onto its IM-1280 image-capturing board. This previously used RGB-to-HSI conversion is defined as the third trichromic system discussed in Ref. 16. The primary difficulty with the Matrox-defined color space arises from the fact that the origin of this color space is not coincident with the white light point. This origin shift was not a problem for the flow situation studied in Ref. 1, wherein all shear vectors were within ±30 deg of the principal flow direction, i.e., no reverse-flow vectors were present. However, given the highly directional color-change-response of SSLCCs to shear vector direction relative to the observer,[12] attempts to employ this color space in the present flow environment, wherein shear vector directions varied over a 360-deg range, led to ambiguities in hue measurements, and, as a consequence, it was abandoned.

Taking advantage of the symmetry of the flowfield, the time-averaged, filtered hue images for $0 \leq \phi_c \leq 180$ deg were mirror-imaged across the plane of symmetry (the X axis) to form a complete $0 \leq \phi_c \leq 360$ deg image set. These hue images were subjected to the image processing and data analysis procedure outlined in Ref. 1 to convert them to an answer set containing a vector-aligned hue value (proportional to shear magnitude) and a vector orientation at every grid-point location on the test surface. The final scaling from vector-aligned hue values to shear magnitudes was accomplished through the use of the calibration curve shown in Fig. 3b. The point measurements of shear magnitude required for calibration purposes were acquired along the X axis through application of the fringe-imaging (oil-drop) skin friction technique.[15] The uncertainty in shear magnitude associated with this point-measurement technique is ±5%.

In the final analysis of the SSLCC data, vector-aligned hue values slightly above the maximum value of the calibration curve were encountered at some surface grid points along and just to either side of the X axis. In such cases, these hue values were equated to the highest shear stress magnitude shown in the calibration curve. Vector-aligned hue values below the lowest nonzero calibration point were dropped from the final surface shear stress vector field.

B. Results

The measured surface shear stress vector distribution is shown in Fig. 4b. This measured data set contains approximately 2×10^5 nonzero vectors, one at every point on a surface grid the resolution of which is 100×100 points/in^2. False color levels are used to represent shear stress magnitudes. Black regions represent the absence of a vector value due either to thresholding at the lowest nonzero calibration point or to the failure to attain an acceptable Gaussian curve fit to the H vs ϕ data set at a particular surface grid point. Vector orientations are illustrated by the vector crosscut profiles drawn every $\Delta X/D = \pm 1$ starting at the Y axis: for clarity, only every fifth vector, spaced $|\Delta Y/D| = 0.15$, is shown in each profile.

Shear magnitude distributions along the X axis and the Y axis are shown in Figs. 5b and 6b, respectively. On the axial profile, Fig. 5b, a shear minimum occurred just to the negative X side of the GSP, coincident with the center of the elliptic stagnation zone noted in the oil-flow pattern of Fig. 2. Because of thresholding applied in the SSLCC method, and/or possibly the unsteadiness observed in this region, a nonzero value of the time-averaged shear magnitude was measured within this small stagnation zone.

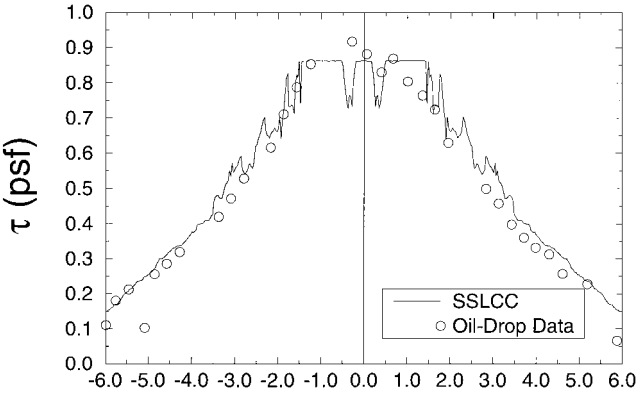

Shear stress vector magnitude

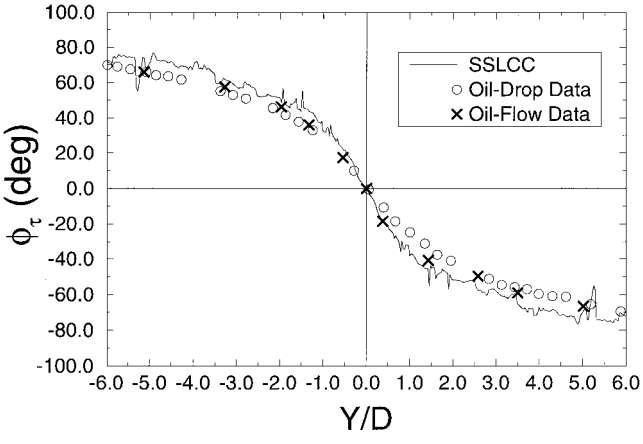

Shear stress vector orientation

Fig. 7 SSLCC measurements vs point measurements on transverse crosscut at *X/D* = 2.

Shear magnitude increased rapidly in all directions emanating from the stagnation zone as the inclined-jet flow turned to align itself with the plate surface and then accelerated outward. Peak shear stresses were measured on both axes within 1–2 D of the GSP. As noted in the preceding section, local shear magnitudes above the maximum value shown in the calibration curve were plotted at that level. Outside of $|X/D| \sim 2$, shear magnitude decreased approximately linearly with distance (Fig. 5), whereas beyond $|Y/D| \sim 2$, it dropped off more rapidly (Fig. 6).

Figure 7 shows continuous measurements from the SSLCC method vs point measurements from the oil-drop method as acquired on a transverse crosscut at $X/D = 2$. None of the oil-drop data shown here were used to generate the SSLCC calibration curve of Fig. 3b. As was the case in Ref. 1, very good overall agreement was noted between shear vector magnitudes and shear vector orientations measured by these two methodologies. On average, shear magnitudes measured by the SSLCC technique were within 4.1% of the oil-drop data, based on the full-range shear value of 0.869 psf, i.e., to within 0.036 psf.

These results demonstrate the capability of the SSLCC method to measure continuous shear stress vector distributions on planar surfaces where shear vectors of all possible orientations are present.

Summary

The impingement of an inclined, axisymmetric, turbulent jet was studied experimentally using pressure-sensitive and shear-sensitive coatings combined with CCD imaging techniques. The results of this research yielded the first-ever consolidated measurements of the continuous pressure and shear stress vector distributions beneath a single, fundamental flowfield. High-spatial-resolution data sets generated with these methods can be used to further define flow physics, as well as to provide standards for computational fluid dynamics code-validation purposes.

Concerning the measurement methodologies themselves, the present results provided another indication that the PSP method can be extended reliably to the measurement of small pressure differences ($< \sim 0.1$ psig) encountered in low-speed atmospheric flows. In addition, these results yielded the first demonstration of the capability of the SSLCC method to reliably measure continuous shear stress vector distributions on planar surfaces where shear vectors of all possible orientations are present.

References

[1]Reda, D. C., Wilder, M. C., Farina, D. J., and Zilliac, G., "New Methodology for the Measurement of Surface Shear Stress Vector Distributions," *AIAA Journal*, Vol. 35, No. 4, 1997, pp. 608–614.

[2]Donaldson, C. D., and Snedeker, R. S., "A Study of Free Jet Impingement, Part 1: Mean Properties of Free and Impinging Jets," *Journal of Fluid Mechanics*, Vol. 45, Pt. 2, 1971, pp. 281–319.

[3]Donaldson, C. D., Snedeker, R. S., and Margolis, D. P., "A Study of Free Jet Impingement, Part 2: Free Jet Turbulent Structure and Impingement Heat Transfer," *Journal of Fluid Mechanics*, Vol. 45, Pt. 3, 1971, pp. 477–512.

[4]Foss, J. F., "Measurements in a Large-Angle Oblique Jet Impingement Flow," *AIAA Journal*, Vol. 17, No. 8, 1979, pp. 801, 802.

[5]Bedii Ozdemir, I., and Whitelaw, J. H., "Impingement of an Axisymmetric Jet on Unheated and Heated Flat Plates," *Journal of Fluid Mechanics*, Vol. 240, 1992, pp. 503–532.

[6]McLachlan, B. G., and Bell, J. H., "Pressure-Sensitive Paint in Aerodynamic Testing," *Experimental Thermal and Fluid Science*, Vol. 10, Oct. 1995, pp. 470–485.

[7]Ardasheva, M. M., Nevskii, L. B., and Pervushin, G. E., "Measurement of Pressure Distribution by Means of Indicator Coatings," *Journal of Applied Mechanics and Technical Physics (USSR)*, Vol. 26, 1985, pp. 469–474.

[8]Kavandi, J., Callis, J., Gouterman, M., Khalil, G., Wright, D., Green, E., Burns, D., and McLachlan, B., "Luminescent Barometry in Wind Tunnels," *Review of Scientific Instruments*, Vol. 61, No. 11, 1990, pp. 3340–3347.

[9]Yuichi, S., Mehta, R. D., and Cantwell, B. J., "Vortical Flow Field Investigation Using the Pressure Sensitive Paint Technique at Low Speed," AIAA Paper 97-0388, Jan. 1997.

[10]Brown, O. C., Mehta, R. D., and Cantwell, B. J., "Low-Speed Flow Studies Using the Pressure Sensitive Paint Measurement Technique," *Proceedings, Advanced Aerodynamic Measurement Technology Symposium* (Seattle, WA), CP-601, AGARD, 1997 (Paper 31).

[11]Fergason, J. L., "Liquid Crystals," *Scientific American*, Vol. 211, Aug. 1964, pp. 76–85.

[12]Reda, D. C., and Muratore, J. J., Jr., "Measurement of Surface Shear Stress Vectors Using Liquid Crystal Coatings," *AIAA Journal*, Vol. 32, No. 8, 1994, pp. 1576–1582.

[13]Reda, D. C., Wilder, M. C., and Crowder, J. P., "Simultaneous, Full-Surface Visualizations of Transition and Separation Using Liquid Crystal Coatings," *AIAA Journal*, Vol. 35, No. 4, 1997, pp. 615, 616.

[14]Haritonidis, J. H., "The Measurement of Wall Shear Stress," *Advances in Fluid Mechanic Measurements*, Springer–Verlag, New York, 1989, pp. 229–261.

[15]Zilliac, G., "Further Developments of the Fringe-Imaging Skin Friction Technique," NASA TM-110425, 1996.

[16]Hay, J. L., and Hollingsworth, D. K., "A Comparison of Trichromic Systems for Use in the Calibration of Polymer-Dispersed Thermochromic Liquid Crystals," *Experimental Thermal and Fluid Science*, Vol. 12, 1996, pp. 1–12.

G. Laufer
Associate Editor